OXFORD
SOT Society of Toxicology
academic.oup.com/toxsci

TOXICOLOGICAL SCIENCES, 177(2), 2020, 483–493

doi: 10.1093/toxsci/kfaa116
Advance Access Publication Date: 16 July 2020
Research Article

2,3′,4,4′,5-Pentachlorobiphenyl Induced Thyrocyte Autophagy by Promoting Calcium Influx via Store-Operated Ca^{2+} Entry

Li Wang,[*] Wenli Xu,[*] Qi Zhou,[*] Bojin Xu,[*] Yunlu Sheng,[†] Minne Sun,[†] Huanhuan Chen,[*] Yucheng Wang,[*] Guoxian Ding,[†] and Yu Duan[*,1]

[*]Department of Endocrinology and [†]Division of Geriatric Endocrinology, The First Affiliated Hospital of Nanjing Medical University, Nanjing 210029, People's Republic of China

[1]To whom correspondence should be addressed at Department of Endocrinology, The First Affiliated Hospital of Nanjing Medical University, 300 Guangzhou Road, Nanjing 210029, People's Republic of China. Fax: +86-25-83780170; E-mail: duanyujsph@163.com

ABSTRACT

PCB118, a 2,3′,4,4′,5-pentachlorobiphenyl, has been shown to destroy thyroidal ultrastructure and induce thyrocyte autophagy. Previously, we reported that PCB118 promoted autophagosome formation *in vivo* and *in vitro*, but more details remain to be revealed. To explore the underlying mechanism by which PCB118 regulates thyrocyte autophagy, Fischer rat thyroid cell line-5 (FRTL-5) cells were exposed to different doses of PCB118 at 0, 0.25, 2.5, and 25 nM for 0–48 h. Western blot analysis of autophagy-related proteins P62, BECLIN1, and LC3 demonstrated that PCB118 induced autophagy formation in dose- and time-dependent manner. Moreover, laser scanning confocal microscopy and flow cytometry showed PCB118 treatment led to time- and dose-dependent increase in intracellular calcium concentration ($[Ca^{2+}]_i$). Additionally, PCB118 promoted store-operated Ca^{2+} entry (SOCE) channel followed by significant increase of ORAI1 and STIM1 protein levels. On the other hand, PCB118 induced thyroidal autophagy via class III β-tubulin (TUBB3)/death-associated protein kinase 2 (DAPK2)/myosin regulatory light chain (MRLC)/autophagy-related 9A (ATG9A) pathway in FRTL-5 cells. Pretreatment with SOCE inhibitor SKF96365 reduced cytosolic Ca^{2+}, ORAI1, STIM1, and BECLIN1 levels as well as LC3 II/LC3 I ratio, while increased P62 expression. SKF96365 also inhibited TUBB3/DAPK2/MRLC/ATG9A pathway in FRTL-5 cells treated by PCB118. Our results provide evidence that PCB118 may induce thyroidal autophagy through TUBB3-related signaling pathway, and these effects are likely to be regulated by calcium influx via SOCE channel.

Key words: PCB118; thyroid; autophagy; calcium influx; SOCE.

Polychlorinated biphenyls (PCBs) are a broad series of environmental organic contaminants with wide applications (Grossman, 2013). PCBs could enter human or animal bodies through food chain due to the characteristics of bio-persistence and lipophilicity (Harmouche-Karaki *et al.*, 2019; Takaguchi *et al.*, 2019). PCBs are toxic to many systems in human body, including immune, nervous, reproductive, and endocrine systems (Coulter *et al.*, 2019; Gaum *et al.*, 2019; Spector *et al.*, 2014).

Exposure to PCBs such as PCB118 could cause structural damage and dysfunction of the thyroid. PCBs have been shown to interfere with thyroidal-related gene expression and thyroid hormone function (Duntas and Stathatos, 2015; Katarzyńska *et al.*, 2015). Fischer rat thyroid cell line-5 (FRTL-5) cells have been confirmed as functional clone cells and behave in a manner similar to normal thyrocytes *in vitro*. FRTL-5 cell line is the most frequent and optimum cell line model used for studying thyrocytes functions related to human pathophysiology due to its accessibility, simplicity, and characteristics of allowing permanent transfections (Medina and Santisteban, 2000; Wen *et al.*, 2017). Therefore, we selected FRTL-5 cell line as the cell model in this study.

As the basic unit of microtubule, Tubulin plays a pivotal role to compose cytoskeleton and sustain cell shape and structure. *Tubb3*, an essential component of Tubulin gene family, endows microtubule with the dynamic characteristics required for rapid responses to extracellular guidance signals. Mutations in *Tubb3* would lead to the reduction of Tubulin, destruction of cytoskeleton and alteration of biochemical properties (Tischfield and Engle, 2010). Death-associated protein kinase 2 (DAPK2) is involved in the formation of autophagosomal structures and regulates the initiation step of autophagy (Geering, 2015). Our recent study showed that low dose PCB118 induced thyroid autophagy by DAPK2 binding to TUBB3, and triggering DAPK2/PKD/VPS34 bypath pathway (Zhou *et al.*, 2019). It is known that DAPK2 could phosphorylate the myosin regulatory light chain (MRLC), the activation state of Myosin II, to promote myosin-dependent trafficking of ATG9-containg vesicles and induce membrane fusion and autophagy (Geering, 2015; Levin-Salomon *et al.*, 2014). However, the link between TUBB3/DAPK2/MRLC/ATG9A pathway and PCB118-induced thyroid autophagy remains to be further investigated.

Importantly, growing evidence has indicated that toxicological mechanism of PCBs is associated with calcium signaling and other ion channels (Pessah *et al.*, 2010). Ca^{2+} plays an essential role in various pathological processes after PCBs exposure (Garcia *et al.*, 2006). Store-operated Ca^{2+} entry (SOCE) channel is a ubiquitous calcium influx pathway in both excitable and non-excitable cells, and includes 2 principal players ORAI1 and STIM1 (Gratschev *et al.*, 2004). Some studies have shown that the perturbation of SOCE channel is a significant toxic mechanism in several cell types (Choi *et al.*, 2016; Lee *et al.*, 2017). However, it also remains unclear whether PCB118 has influence on SOCE channel in FRTL-5 cells, even more the potential role of SOCE in PCB118-induced autophagy.

Therefore, this study aimed to identify the relationship among PCB118, SOCE channel and thyrocyte autophagy, and disclosing the mechanism of PCB118-induced autophagy in thyroid FRTL-5 cells.

MATERIALS AND METHODS

Reagents. PCB118 (purity of 100%; CAS no. 31508-00-6) was obtained from Accu Standard (USA). Fluo-3/AM was acquired from Beyotime (China). SKF96365 was obtained from Apexbio Technology (USA) and the final working dose of SKF96365 was 10 μM which did not affect cellular growth by viability tests (data not shown).

Cell culture and treatment. FRTL-5 cells were incubated in modified Ham's F12 medium (including 0.1245 g/l calcium chloride), and exposed to low-dose PCB118 (0–25 nM), which did not influence cell viability and apoptosis according to previous report (Yang *et al.*, 2015).

Western blot analysis. Western blot analysis was conducted following previously described protocol (Yang *et al.*, 2015). The primary antibodies were against GAPDH, P62, LC3, BECLIN1, TUBB3, MRLC, phospho-MRLC (P-MRLC), ATG9A, STIM1 (all from CST, USA), ORAI1 (Absin, China), and DAPK2 (Biorbyt, UK). The secondary antibodies were purchased from Vector Laboratories (USA). The protein bands were visualized by chemiluminescence reagent (ThermoFisher Scientific, USA) and qualified using Image-J software (National Institute of Health, USA).

Quantitative real-time PCR. Total RNA was isolated from thyrocyte using RNAiso Plus (Takara, Japan), and cDNA was synthesized using PrimeScript RT Master Mix Kit (Takara). Quantitative real-time PCR was performed using SYBR-Green kit on StepOnePlus system (Applied Biosystems, USA). Primer sequences of *Tubb3*, *Dapk2*, non-muscle myosin heavy chain IIA (*NMMHC-IIA*), *Atg9a* and *β-actin* were listed in Supplementary Table 1. Relative mRNA levels were calculated using $2^{-\Delta\Delta CT}$ method.

Intracellular calcium level measurement. Total cytosolic calcium levels were detected with Fluo-3/AM probe. Cells were inoculated in 6-well plates and treated by PCB118. The cells were then incubated with 2 μM Fluo-3/AM in serum-free medium at 37°C for 0.5 h, washed with calcium-free PBS 3 times, and detected by flow cytometer (BD Biosciences). Ca^{2+} levels were quantified using Flow-Jo V10 software (Tree Star, USA).

In addition, the cells were incubated for 30 min with calcium-free PBS containing 5 μM Fluo-3/AM, washed with calcium-free PBS and then stained by Hoechst 33342 (Beyotime, China) for 20 min. Next, cells were observed under laser scanning confocal microscopy (LSCM). Cytosolic Ca^{2+} levels were quantified using Image-J.

Small-interfering RNA. *Tubb3*-, *Dapk2*-, *NMMHC-IIA*-targeting small-interfering RNAs (siRNAs), and negative control (NC) siRNA were designed with the sequences listed in Supplementary Table 2, and transfected into FRTL-5 cells using Lipofectamine 2000 (Invitrogen, USA). Then, cells were exposed to 25 nM PCB118 for 24 h.

Lentiviral vector. Lentiviral vector Lv-Tubb3 for *Tubb3* overexpression was constructed by GenePharma (Shanghai, China). The cells were infected with Lv-Tubb3 or NC lentivirus at multiplicity of infection (MOI) of 100 for 72 h, and then treated with 25 nM PCB118 for 24 h.

Statistics. All results from at least triplicate experiments were shown as mean ± SEM, and analyzed by 1-way analysis of variance (ANOVA) or *t* test, Sidak's multiple comparisons test was used for post-hoc analysis after ANOVA, and $p < .05$ indicated statistical significance.

RESULTS

Pcb118-Induced Thyrocyte Autophagy in Dose- and Time-Dependent Manner

To investigate how PCB118 induced thyrocyte autophagy, we treated FRTL-5 cells with PCB118 at the range of 0.25, 2.5, and 25 nM. The expression of autophagy markers BECLIN1, LC3 and P62 were analyzed by Western blot analysis. After exposure to PCB118, LC3 II/LC3 I ratio, and BECLIN1 level significantly enhanced, whereas P62 protein expression significantly attenuated dose-dependently ($p < .01$, Figure 1a).

Furthermore, 0–48 h of exposure to 25 nM PCB118 showed that BECLIN1 level and LC3 II/LC3 I ratio significantly increased over the first 36 h but decreased in the 48 h group after PCB118 exposure (Figure 1b). Meanwhile, P62 protein expression showed significant decrease from 6 to 36 h ($p < .01$), minimized at 36 h, and then slightly increased at 48 h ($p < .01$, Figure 1b). These data suggested that PCB118 enhanced autophagy in concentration- and time-dependent manner in FRTL-5 cells.

Pcb118-Elevated Intracellular Calcium in Dose- and Time-Dependent Manner

To demonstrate the effects of PCB118 on cytosolic calcium levels, we employed flow cytometry to detect Ca^{2+}-sensitive dye

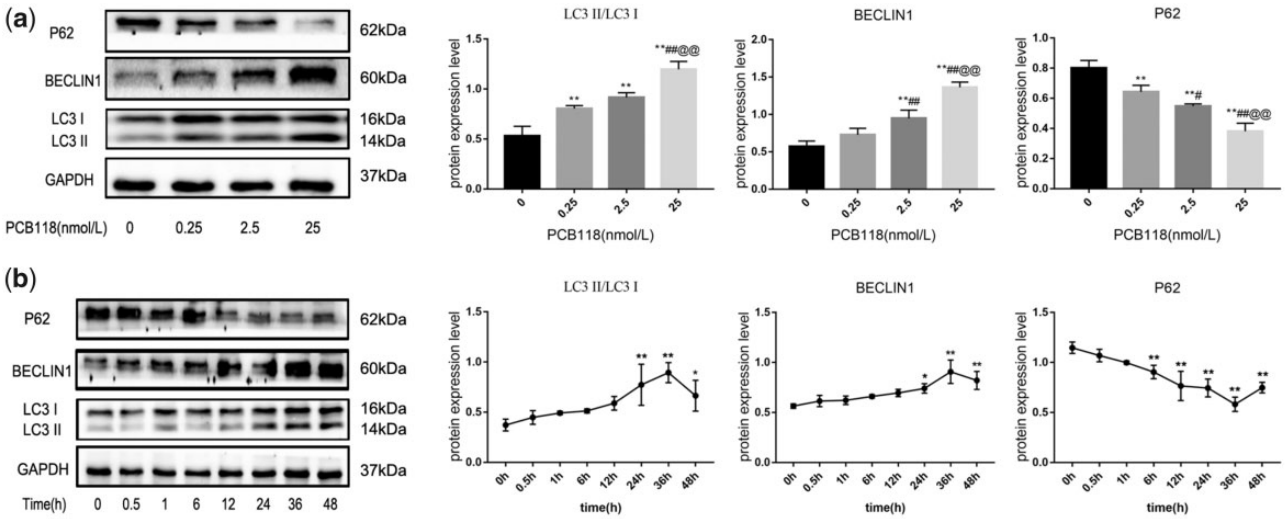

Figure 1. PCB118 promoted autophagy formation in FRTL-5 cells in dose- and time-dependent manner. The cells were exposed to 0–25 nM PCB118 for 24 h (a) and 25 nM PCB118 for 0–48 h (b). Representative protein bands (left) and densitometric analysis of P62, BECLIN1 and LC3 protein levels (right). Results are shown as mean ± SEM ($n = 3$–6). $^{**}p < .01$ versus vehicle, #$p < .05$, ##$p < .01$ versus 0.25 nM group, @@$p < .01$ versus 2.5 nM group (a); $^{*}p < .05$, $^{**}p < .01$ versus 0 h control group (b), 1-way ANOVA followed by Sidak's multiple comparisons test. GAPDH was loading control.

Fluo-3/AM. The results indicated that PCB118 increased $[Ca^{2+}]_i$ in a dose-dependent manner, and showed significant difference in 25 nM group compared with the control group ($p < .01$, Figs. 2a and 2b). Furthermore, in cells exposed to 25 nM PCB118, Ca^{2+} levels enhanced at the first 24 h while declined at 36 and 48 h, with significant difference from 6 to 36 h compared with 0 h group ($p < .01$, Figs. 2c and 2d). These data indicated that PCB118 increased intracellular Ca^{2+} levels in dose- and time-dependent manner.

To further corroborate such findings, we utilized Fluo-3/AM probe to monitor intracellular Ca^{2+} under confocal microscope. We found that cytosolic Ca^{2+} levels significantly enhanced in all PCB118-treated groups, and showed significant difference between 0.25 nM group and 2.5, 25 nM group, respectively ($p < .01$, Figs. 2e and 2f). For cells incubated with 25 nM PCB118, $[Ca^{2+}]_i$ levels increased over the first 24 h and then gradually declined, with statistical difference in 6, 12, 24, 36, and 48 h group ($p < .01$, Figs. 2g and 2h). Collectively, $[Ca^{2+}]_i$ showed dose- and time-dependent change in FRTL-5 cells after PCB118 stimulation.

Pcb118-Promoted Calcium Influx via SOCE Channel in FRTL-5 Cells

In order to determine the role of SOCE channel, we performed Western blot analysis of ORAI1 and STIM1. Compared with control group, ORAI1 and STIM1 protein levels were significantly enhanced by 24 h treatment with 25 nM PCB118 ($p < .01$, Figs. 3a–c). However, pretreatment with SKF96365, the inhibitor of SOCE, significantly reduced the expression of ORAI1 and STIM1 ($p < .01$, Figs. 3d–f). Additionally, PCB118-induced increase of cytosolic Ca^{2+} levels was attenuated by SKF96365 ($p < .01$, Figs. 3g and 3h). In summary, these results indicated that SOCE channel may play a significant role in PCB118-induced calcium influx.

Pcb118-Activated Autophagy-Related Pathway in FRTL-5 Cells

Tubb3 mRNA and protein levels reduced significantly in PCB118-treated cells ($p < .01$, Figure 4). *Dapk2* mRNA and protein levels exhibited dose-dependent increase in 0.25 and 2.5 nM groups, and reduced slightly in 25 nM group ($p < .01$, Figure 4). In addition, *NMMHC-IIA* mRNA level, which represents gene expression of MRLC, gradually increased in 0.25 and 2.5 nM groups and decreased slightly in 25 nM group (Figure 4a). Elevated P-MRLC/MRLC ratio was significantly correlated with higher concentrations of PCB118, and showed significant increase in 25 nM group compared with control ($p < .05$, Figure 4b). Moreover, both *Atg9a* mRNA and protein levels significantly increased in 2.5 and 25 nM groups compared with control ($p < .01$, Figure 4).

To confirm the function of these molecules in autophagy of FRTL-5 cells, we employed siRNAs or lentivirus vector for gene knockdown or overexpress. *siTubb3* could inhibit PCB118-induced phosphorylation/activation of MRLC and upregulation of DAPK2 and ATG9A ($p < .05$, Figs. 5a–c). Similarly, *siDapk2* significantly decreased the phosphorylation of MRLC and the expression of ATG9A in FRTL-5 cells exposed to PCB118 ($p < .01$, Figs. 5b and 5c). Moreover, ATG9A protein expression was significantly inhibited after knockdown of *NMMHC-IIA* compared with PCB118-NC group ($p < .01$, Figure 5c).

Consistently, Lv-Tubb3-mediated *Tubb3* overexpression could enhance PCB118-induced DAPK2 upregulation ($p < .01$, Figure 5d). Furthermore, *Tubb3* overexpression increased P-MRLC/MRLC ratio and ATG9A protein levels compared with PCB118-NC group ($p < .01$, Figs. 5e and 5f). Taken together, these data demonstrated that PCB118-activated TUBB3/DAPK2/MRLC/ATG9A pathway in FRTL-5 cells.

Activation of Thyrocyte Autophagy by PCB118 Is SOCE Dependent

We wondered whether SOCE mediated calcium influx could be responsible for thyrocyte autophagy. Pretreated cells with SKF96365 could reduce the level of BECLIN1 and LC3 II/LC3 I ratio compared with 25 nM PCB118 alone group ($p < .01$, Figs. 6a–c). Under the same treated condition, P62 protein was significantly enhanced and statistical difference was found between PCB118 with SKF96365 group and PCB118 control group ($p < .05$, Figs. 6a and 6d).

Next, we detected the effects of SOCE channel on autophagy-related pathway. Western blot analysis showed that protein levels of TUBB3, DAPK2, and ATG9A as well as P-MRLC/MRLC ratio significantly reduced in FRTL-5 cells pretreated with

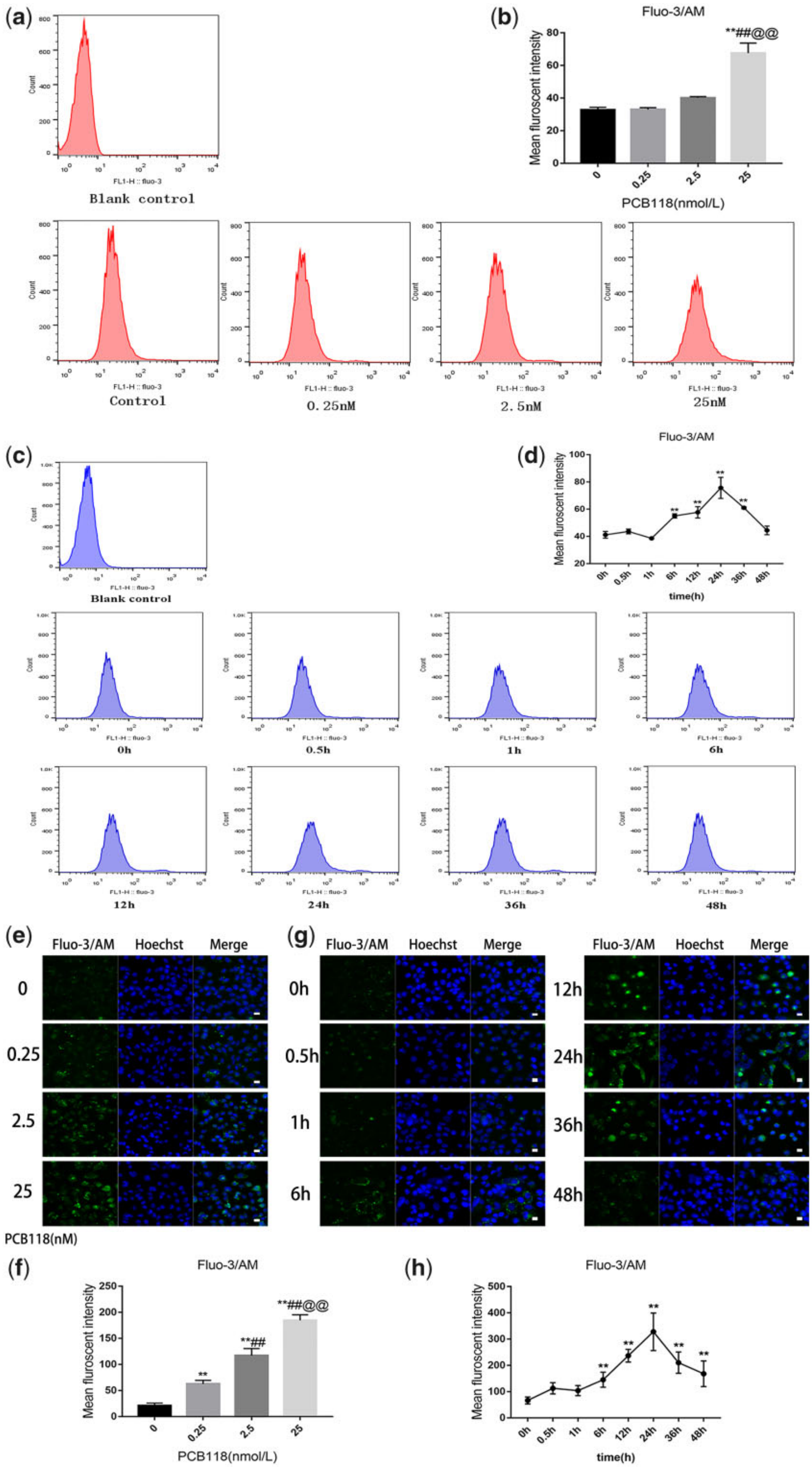

Figure 2. Intracellular calcium levels in cells following PCB118 exposure. FRTL-5 cells were treated with PCB118 (0–25 nM) for 24 h (a, b, e, f) or 25 nM PCB118 for 0–48 h (c, d, g, h) and then analyzed with Flow-3/AM via flow cytometry (a–d) or LSCM (e–h). (e, g) Confocal images. Flow-3/AM was indicator of cytosolic Ca^{2+} (green). Hoechst 33342 was used for nuclear staining (blue). Scale bar, 20 μm. (b, d, f, h) Relative mean fluorescent intensity (MFI). Data are presented as mean ± SEM ($n = 3$–6). $^{**}p < .01$ versus control group, $^{\#\#}p < .01$ versus 0.25 nM group, @@$p < .01$ versus 2.5 nM group (b, f); $^{**}p < .01$ versus 0 h control group (d, h), 1-way ANOVA followed by Sidak's multiple comparisons test.

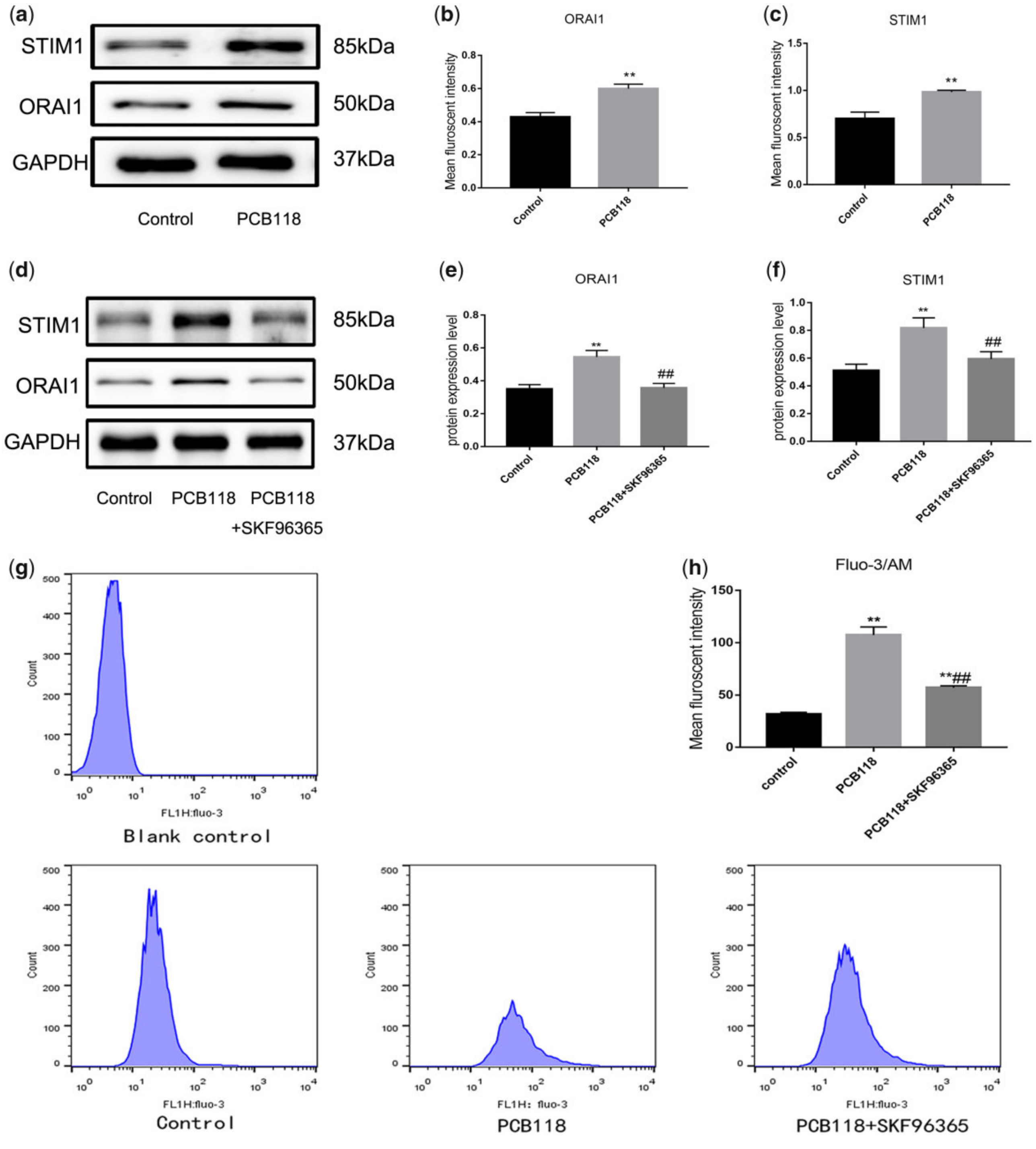

Figure 3. PCB118 induced calcium influx via SOCE channel in FRTL-5 cells. Cells were stimulated with 25 nM PCB118 for 24 h and ORAI1 and STIM1 were detected by Western blot analysis (a–c). Cells were pretreated with 10 μM SKF96365 for 1 h and then stimulated with 25 nM PCB118 for 24 h for Western blot (d–f) and flow cytometry analysis (g, h). (a, d) Representative protein bands. (b, c, e, f) Quantification of protein bands. (h) Quantification of MFI by Flow-3/AM (2 μM). Mean ± SEM ($n = 3$–6). **$p < .01$ versus vehicle; ##$p < .01$ versus 25 nM PCB118 group, student's t test (b, c) and 1-way ANOVA followed by Sidak's multiple comparisons test (e, f, h).

SKF96365 compared with FRTL-5 cells treated with PCB118 alone (Figs. 6e–i).

DISCUSSION

As a group of widespread endocrine-disrupting compounds (EDCs), PCBs have been investigated for their toxic effects in many aspects in endocrine system (Maqbool *et al.*, 2016). PCB118 is one of the most persistent PCBs congeners and has been detected in human breast milk and human tissues (Tarkowski, 1996). PCB118 is also one of the 9 PCB congeners most closely related to thyroid dysfunction (Bloom *et al.*, 2003), and its pollution is widespread in soil, water, and the aquatic organisms of the Yangtze River Delta region of China (Zhao *et al.*, 2009). PCB118 could be used as the typical and direct indicator of total PCBs in the environment (Kang *et al.*, 2008; Rudge *et al.*, 2012).

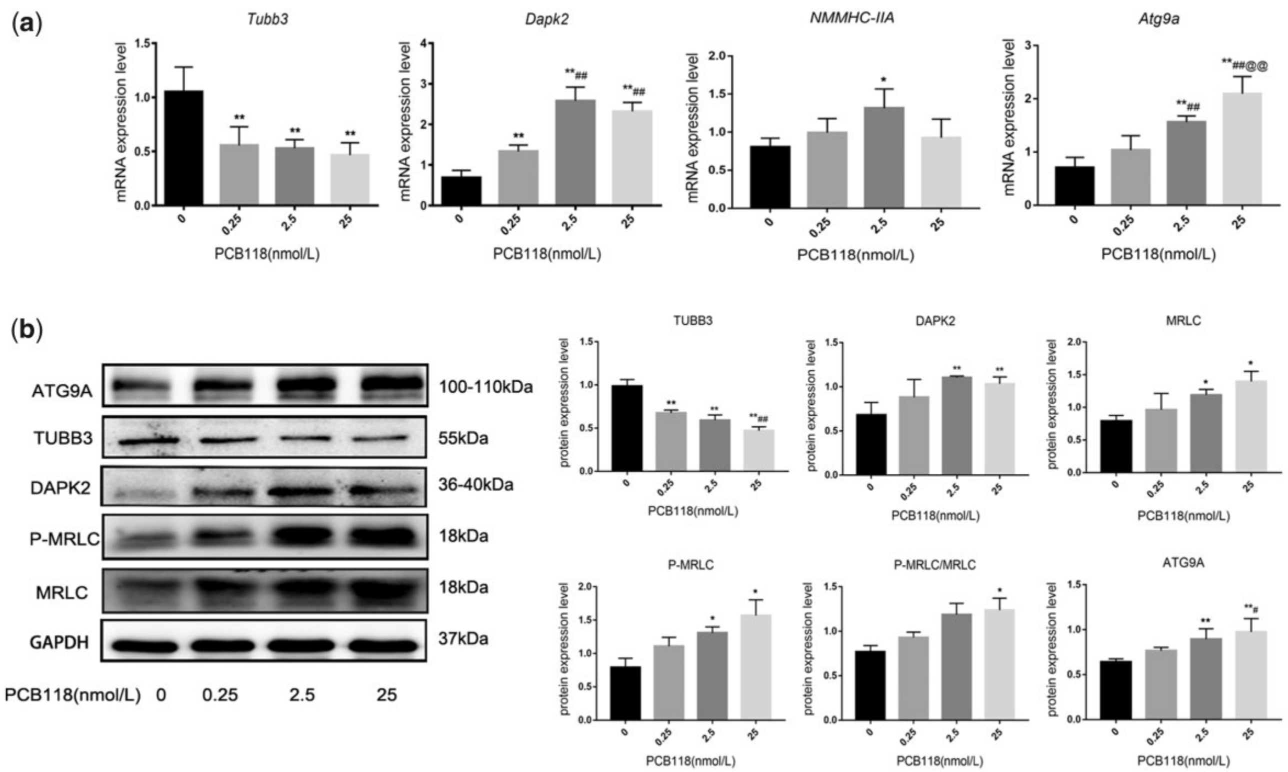

Figure 4. PCB118 regulated DAPK2, TUBB3, MRLC, and ATG9A expression in FRTL-5 cells. a, mRNA levels were detected by PCR. *p <.05, **p <.01 versus vehicle, ##p <.01 versus 0.25 nM group, @@p <.01 versus 2.5 nM group. b, Western blot analysis of DAPK2, TUBB3, MRLC, P-MRLC and ATG9A protein levels. Representative protein bands (left) and densitometric analysis of protein bands (right). Mean ± SEM (n = 3–6). *p <.05, **p <.01 versus vehicle; #p <.05, ##p <.01 versus 0.25 nM group, 1-way ANOVA followed by Sidak's multiple comparisons test.

Importantly, the thyroid gland is highly susceptible to the effect of PCBs. Our previous studies *in vivo* revealed that PCB118 could damage thyroid structure even at a minimal concentration of 10 μg/kg/day, and no clinical symptoms or behavioral disturbances occurred in Wistar rats with chronic low-dose exposure to PCB118 (10, 100, and 1000 μg/kg/day for 13 weeks) (Tang *et al.*, 2013; Xu *et al.*, 2016). On the other hand, the concentration of PCB118 we selected from 0.25 to 25 nM in the study did not affect cell viability or apoptosis (Yang *et al.*, 2015), and was lower than the doses used in other studies on the effects of PCBs on nervous and endocrine system dysfunction (Dickerson *et al.*, 2009; Merritt and Foran, 2007; Sánchez-Alonso *et al.*, 2003). A general regional investigation had been detected that the median dose of PCB118 was 45 pg/ml (1.38 nM) and ranged between 120 and 1580 pg/ml (0.38–4.84 nM) in maternal blood collected from 44 women living in Belgium (Covaci *et al.*, 2002), and the doses were similar to the doses used in our experiment (0.25, 2.5, and 25 nM) *in vitro*. Besides, a polluted regional investigation showed that circulating concentration of PCBs reached to 3×10^3 nM in people exposed to PCBs (Wassermann *et al.*, 1979) and the dose much higher than that in thyroid FRTL-5 cells in this study. In previous studies, such low dose of PCB118 could interfere serum thyroid hormones and decrease sodium/iodide symporter (NIS) and thyroglobulin (TG) gene expression both in rat thyroid (FRTL-5) cells and human thyroidal epithelial cells (HETCs) (Guo *et al.*, 2015; Yang *et al.*, 2015). However, few investigations on PCBs-related autophagy in the thyroid have been reported.

As a conserved catabolic degradation/recycling process, autophagy is essential to cellular homeostasis (Klionsky, 2007). In a recent study, we found that the quantity of autophagosomes significantly increased in rat thyroid tissues with PCB118 exposure in a dose-dependent manner. Additionally, it was also found that red fluorescent spot which labeled LC3 II antibody was gradually stained and becoming strongly in dose-related pattern in FRTL-5 cells exposed to PCB118. Such results disclosed that PCB118-induced thyroidal autophagy may be mediated by an alternative pathway *in vivo* and *in vitro* (Zhou *et al.*, 2019). However, the dominant thyroidal autophagy-related approach PCB118 related is still unclear, and furthermore its key regulator mediated such autophagosome formation remains elusive.

LC3 conversion (LC3 I to LC3 II) reflects autophagic activity, whereas BECLIN1 participates in the regulation of autophagosome formation and maturation by interacting with VPS34 (Maejima *et al.*, 2016; Mizushima and Yoshimori, 2007). Therefore, we detected the changes of autophagy-associated markers including BECLIN1, LC3 in thyroid FRTL-5 cells after PCB118 exposure. Our results showed that BECLIN1 level and LC3 II/LC3 I ratio increased dose- and time-dependently, and maximized in FRTL-5 cells treated with 25 nM PCB118 for 36 h. P62 protein could regulate autophagy influx and autolysosomal lytic activity by linking polyubiquitinated proteins with autophagic machinery, and its level would be reduced during autophagy (Bjorkoy *et al.*, 2005). Consistently, we found that PCB118 decreased P62 level in FRTL-5 cells. Taken together, these findings confirmed distinct autophagy phenomena were occurred in the highest dose group at the time of 36 h in FRTL-5 cells when PCB118 stimulated.

The association between calcium and autophagy has been extensively investigated. The changes in $[Ca^{2+}]_i$ affect a large range of cellular processes, such as cell motility, DNA synthesis,

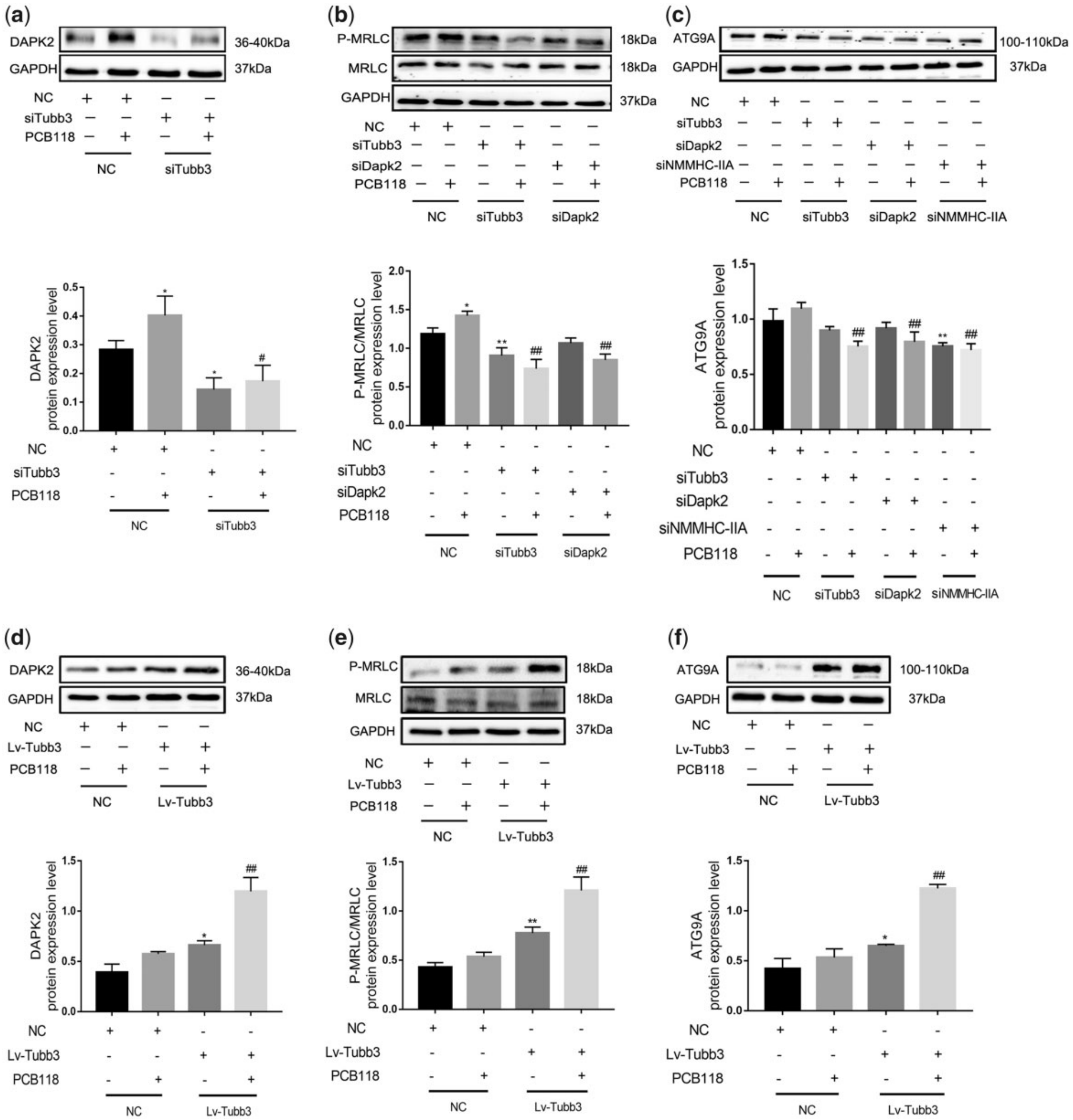

Figure 5. TUBB3 regulated DAPK2-MRLC-ATG9A pathway in FRTL-5 cells. DAPK2, P-MRLC/MRLC, and ATG9A protein levels in cells exposed to PCB118 after treatment with siRNAs (a–c) or Lv-Tubb3 (d–f). Mean ± SEM ($n = 3$–6). (a–c) NC, negative control, non-targeting siRNA, *$p < .05$, **$p < .01$, versus NC group, #$p < .05$, ##$p < .01$, versus PCB118-NC group; (d–f) NC, negative control, blank lentivirus-vector, *$p < .05$, **$p < .01$ versus NC group, ##$p < .01$ versus PCB118-NC group, 1-way ANOVA followed by Sidak's multiple comparisons test.

gene transcription, apoptosis, and autophagy (Becchetti and Arcangeli, 2010; Bootman et al., 2018; Orrenius et al., 2003). In our study, both laser scanning confocal microscopy and flow cytometry analysis showed that PCB118 increased intracellular calcium levels in time- and dose-dependent way, and $[Ca^{2+}]_i$ maximized in 25 nM group with 24 h treatment. Interestingly, PCB118-induced $[Ca^{2+}]_i$ and autophagy seemed to display a coincident pace from 6 to 24 h, suggesting some intimate relationship between Ca^{2+} influx and autophagosome in FRTL-5 cells exposed to PCB118.

It was postulated that SOCE channel plays an essential role in regulating calcium homeostasis in rat thyroid FRTL-5 cells (Tornquist et al., 2002). SOCE includes the major regulator STIM1 and the main pore-forming Ca^{2+} channel subunit ORAI1 (Ambudkar et al., 2017). In this study, we found that PCB118 upregulated ORAI1 and STIM1 protein expression in FRTL-5 cells. In addition, pretreatment with SOCE inhibitor SKF96365 could significantly suppress the expression of STIM1and ORAI1 and synchronously inhibit intracellular Ca^{2+} levels. It was reported that the activation of SOCE was initiated by IP3 binding

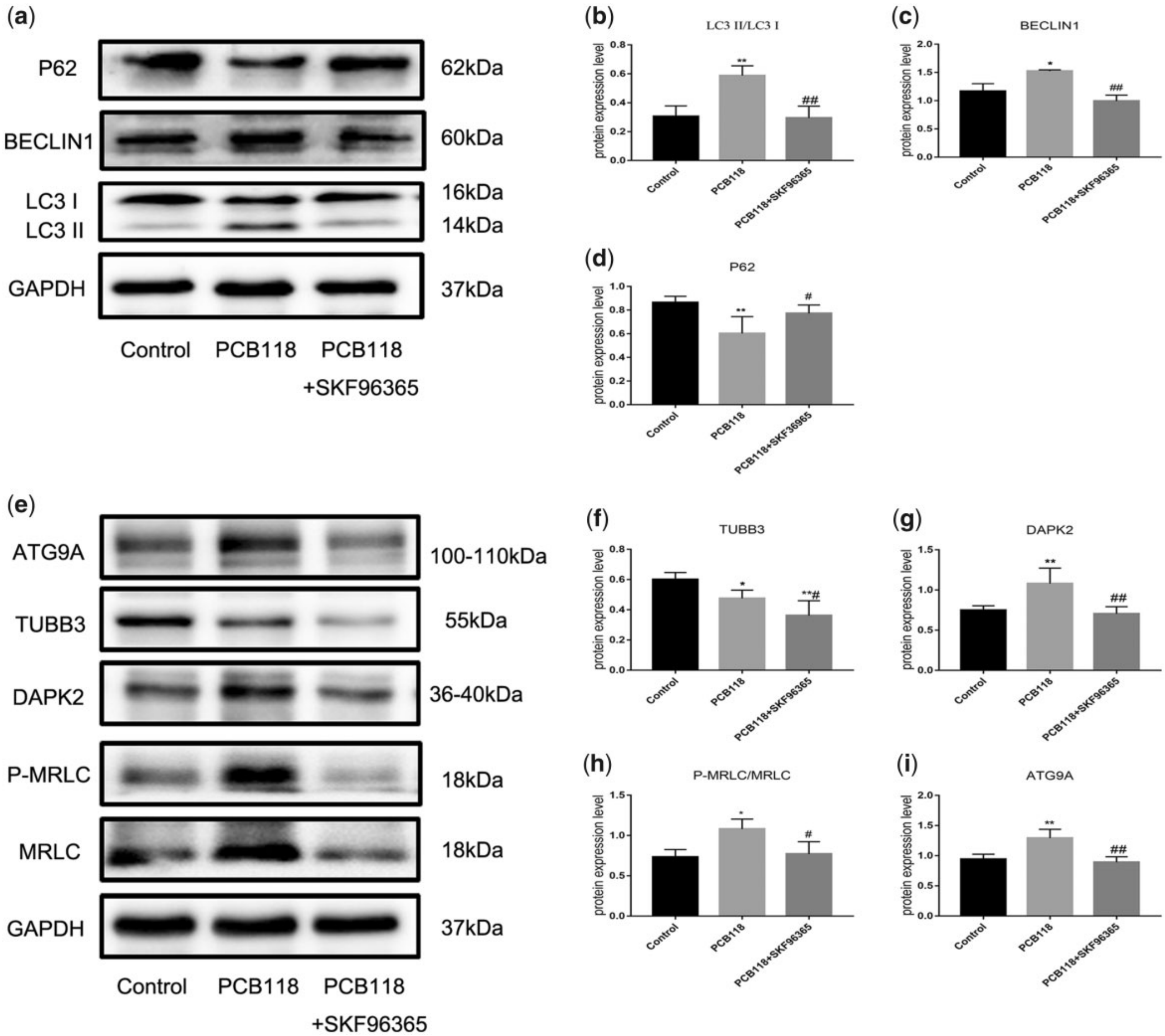

Figure 6. PCB118-induced autophagy and autophagy-related pathway were inhibited by SKF96365. Cells were pretreated with SKF96365 (10 μM) for 1 h and then stimulated with 25 nM PCB118 for 24 h. P62, BECLIN1, LC3, DAPK2, TUBB3, P-MRLC, MRLC, and ATG9A levels were detected by Western blot analysis (a–i). Representative protein bands (a, e) and quantification of protein bands (b–d and f–i). Mean ± SEM ($n = 3$–6). *$p < .05$, **$p < .01$ versus control group; #$p < .05$, ##$p < .01$ versus 25 nM PCB118 group, 1-way ANOVA followed by Sidak's multiple comparisons test.

to its receptor in cytosolic Ca^{2+} pools, which then induced Ca^{2+} release and profound entry of extracellular Ca^{2+} influx via activated SOCE channel (Abdelazeem *et al.*, 2019). In addition, similar investigations confirmed that PCBs could influence Ca^{2+} signaling and Ca^{2+} entry (Lee *et al.*, 2017). Our results revealed that PCB118-induced $[Ca^{2+}]_i$ in FRTL-5 cells was primarily caused by activated SOCE channel.

Previously, we reported that PCB118-induced thyroidal autophagosome was mediated by TUBB3/DAPK2/PKD/VPS34 cascade *in vivo* and *in vitro* (Zhou *et al.*, 2019). However, in that study, the phosphorylation of VPS34 was suppressed only by *siPkd*, suggesting that such pathway may play a partial role in thyroidal autophagy. β-Tubulin, a family of cytoskeleton genes, including TUBB3 has been identified as a novel DAPK2-interacting partner (Isshiki *et al.*, 2015; Zhou *et al.*, 2019). DAPK2 belongs to CaM-regulated serine/threonine (Ser/Thr) kinases family and mediates diverse cellular activities, such as membrane blebbing, inflammation, apoptosis, and autophagy (Geering, 2015). In this study, we found that DAPK2 was upregulated by PCB118, and *NMMHC-IIA*, phosphorylated MRLC, and ATG9A levels consistently increased in cells with PCB118 exposure. Furthermore, in the verification of the pathway, we found that *siTubb3*, *siDapk2*, and *siNMMHC-IIA* could ordinally inhibit the downstream targets and block the pathway in FRTL-5 cells, whereas overexpression of *Tubb3* would successively promote DAPK2, phosphorylation of MRLC, and ATG9A levels. Similar studies confirmed that the activation of DAPK contributed to autophagy formation and induced membrane blebbing by phosphorylating MRLC and tracking ATG9-containing vesicles to the autophagosome formation sites (Bialik *et al.*, 2011; Gilad *et al.*, 2014; Inbal *et al.*, 2002; Tang and Chen, 2011). Our investigations demonstrated that exposure to PCB118 caused abnormal expression of TUBB3, DAPK2, MRLC, and ATG9A, and TUBB3/DAPK2/MRLC/ATG9A pathway could be the principal pathway that mediates PCB118-induced autophagy in FRTL-5 cells.

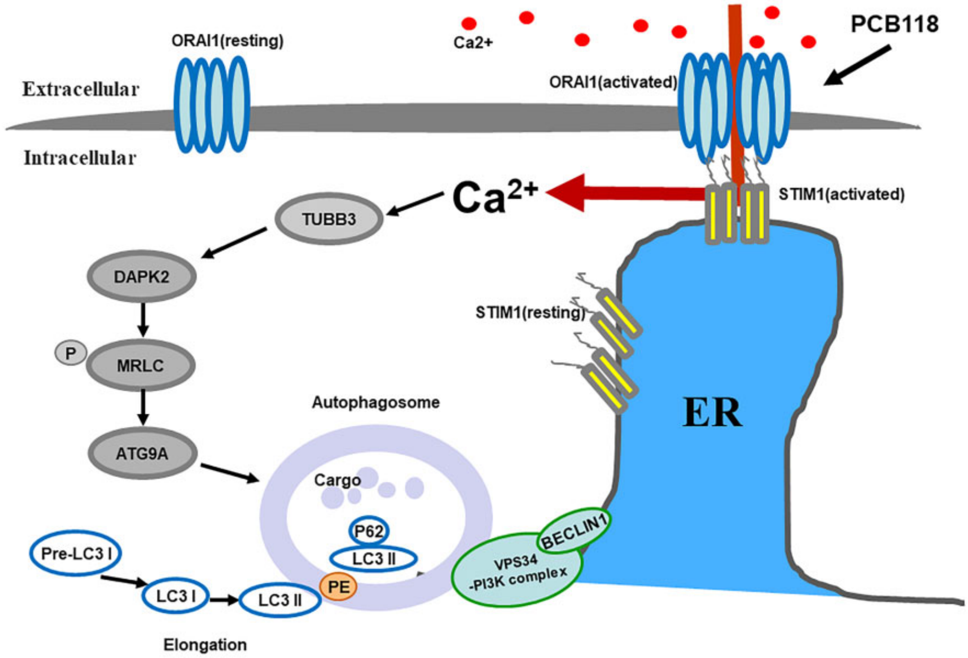

Figure 7. Functional diagram of SOCE-mediated autophagy-related pathway in thyrocyte. PCB118 activates SOCE channel by binding STIM1 to ORAI1, promotes calcium influx, and triggers TUBB3/DAPK2/MRLC/ATG9A pathway to initiate thyrocyte autophagy. ER, Endoplasmic reticulum; PE, phosphatidylethanolamine.

SOCE-mediated $[Ca^{2+}]_i$ was associated with various signaling pathways regulating autophagy (Ali *et al.*, 2017; Yang *et al.*, 2017; Zhu *et al.*, 2018). In this study, we showed that pretreatment with SKF96365 reduced the expression of BECLIN1 and the ratio of LC3 II to LC3 I and enhanced P62 protein level, whereas TUBB3, DAPK2, phosphorylated MRLC, and ATG9A levels were significantly suppressed in cells exposed to PCB118. These results suggested that SOCE may contribute to PCB118-induced autophagy through regulating TUBB3-related pathway in FRTL-5 cells (Figure 7). As for details how PCB118 is internalized in thyrocyte and regulates SOCE need further investigations.

In summary, our results provide evidence that exposure to PCB118 promotes calcium influx via SOCE channel, which then triggers TUBB3-related pathway to initiate thyrocyte autophagy.

SUPPLEMENTARY DATA

Supplementary data are available at *Toxicological Sciences* online.

AUTHOR CONTRIBUTIONS

L.W. and B.X. designed the study; L.W., W.X., Q.Z., and M.S. performed the experiments; Y.S., H.C., and Y.W. analyzed the data; L.W. wrote the manuscript; G.D. edited this article; and Y.D. supervised the study. All authors read and approved the final manuscript.

ACKNOWLEDGMENTS

The authors thank many individuals for their technical assistance in the process of this research.

FUNDING

National Natural Science Foundation of China (81670724 to Y.D.).

DECLARATION OF CONFLICTING INTERESTS

The authors declared no potential conflicts of interest with respect to the research, authorship, and/or publication of this article.

REFERENCES

Abdelazeem, K. N. M., Droppova, B., Sukkar, B., Al-Maghout, T., Pelzl, L., Zacharopoulou, N., Ali Hassan, N. H., Abdel-Fattah, K. I., Stournaras, C., and Lang, F. (2019). Upregulation of ORAI1 and STIM1 expression as well as store-operated Ca(2+) entry in ovary carcinoma cells by placental growth factor. *Biochem. Biophys. Res. Commun.* **512**, 467–472.

Ali, E. S., Rychkov, G. Y., and Barritt, G. J. (2017). Metabolic disorders and cancer: Hepatocyte store-operated Ca(2+) channels in nonalcoholic fatty liver disease. *Adv. Exp. Med. Biol.* **993**, 595–621.

Ambudkar, I. S., de Souza, L. B., and Ong, H. L. (2017). Trpc1, ORAI1, and STIM1 in SOCE: Friends in tight spaces. *Cell Calcium* **63**, 33–39.

Becchetti, A., and Arcangeli, A. (2010). Integrins and ion channels in cell migration: Implications for neuronal development, wound healing and metastatic spread. *Adv. Exp. Med. Biol.* **674**, 107–123.

Bialik, S., Pietrokovski, S., and Kimchi, A. (2011). Myosin drives autophagy in a pathway linking ATG1 to ATG9. *Embo J.* **30**, 629–630.

Bjorkoy, G., Lamark, T., Brech, A., Outzen, H., Perander, M., Overvatn, A., Stenmark, H., and Johansen, T. (2005). P62/sqstm1 forms protein aggregates degraded by autophagy and has a protective effect on huntingtin-induced cell death. *J. Cell Biol.* **171**, 603–614.

Bloom, M. S., Weiner, J. M., Vena, J. E., and Beehler, G. P. (2003). Exploring associations between serum levels of select organochlorines and thyroxine in a sample of New York state sportsmen: The New York state angler cohort study. *Environ. Res.* **93**, 52–66.

Bootman, M. D., Chehab, T., Bultynck, G., Parys, J. B., and Rietdorf, K. (2018). The regulation of autophagy by calcium signals: Do we have a consensus? *Cell Calcium* **70**, 32–46.

Choi, S.-Y., Lee, K., Park, Y., Lee, S.-H., Jo, S.-H., Chung, S., and Kim, K.-T. (2016). Non-dioxin-like polychlorinated biphenyls inhibit g-protein coupled receptor-mediated Ca2+ signaling by blocking store-operated Ca2+ entry. *PLoS One* **11**, e0150921.

Coulter, D. P., Huff Hartz, K. E., Sepulveda, M. S., Godfrey, A., Garvey, J. E., and Lydy, M. J. (2019). Lifelong exposure to dioxin-like PCBs alters paternal offspring care behavior and reduces male fish reproductive success. *Environ. Sci. Technol.* **53**, 11507–11514.

Covaci, A., Jorens, P., Jacquemyn, Y., and Schepens, P. (2002). Distribution of PCBs and organochlorine pesticides in umbilical cord and maternal serum. *Sci. Total Environ.* **298**, 45–53.

Dickerson, S. M., Guevara, E., Woller, M. J., and Gore, A. C. (2009). Cell death mechanisms in gt1-7 gnrh cells exposed to polychlorinated biphenyls pcb74, pcb118, and pcb153. *Toxicol. Appl. Pharmacol.* **237**, 237–245.

Duntas, L. H., and Stathatos, N. (2015). Toxic chemicals and thyroid function: Hard facts and lateral thinking. *Rev. Endocr. Metab. Disord.* **16**, 311–318.

Garcia, A. G., Garcia-De-Diego, A. M., Gandia, L., Borges, R., and Garcia-Sancho, J. (2006). Calcium signaling and exocytosis in adrenal chromaffin cells. *Physiol. Rev.* **86**, 1093–1131.

Gaum, P. M., Gube, M., Esser, A., Schettgen, T., Quinete, N., Bertram, J., Putschogl, F. M., Kraus, T., and Lang, J. (2019). Depressive symptoms after PCB exposure: Hypotheses for underlying pathomechanisms via the thyroid and dopamine system. *Int. J. Environ. Res. Public Health* **16**, 950.

Geering, B. (2015). Death-associated protein kinase 2: Regulator of apoptosis, autophagy and inflammation. *Int. J. Biochem. Cell Biol.* **65**, 151–154.

Gilad, Y., Shiloh, R., Ber, Y., Bialik, S., and Kimchi, A. (2014). Discovering protein-protein interactions within the programmed cell death network using a protein-fragment complementation screen. *Cell Rep.* **8**, 909–921.

Gratschev, D., Blom, T., Bjorklund, S., and Tornquist, K. (2004). Phosphatase inhibition reveals a calcium entry pathway dependent on protein kinase A in thyroid frtl-5 cells: Comparison with store-operated calcium entry. *J. Biol. Chem.* **279**, 49816–49824.

Grossman, E. (2013). Nonlegacy PCBs: Pigment manufacturing by-products get a second look. *Environ. Health Perspect.* **121**, A86–93.

Guo, H., Yang, H., Chen, H., Li, W., Tang, J., Cheng, P., Xie, Y., Liu, Y., Ding, G., Cui, D., *et al*. (2015). Molecular mechanisms of human thyrocyte dysfunction induced by low concentrations of polychlorinated biphenyl 118 through the Akt/FoxO3a/NIS pathway. *J. Appl. Toxicol.* **35**, 992–998.

Harmouche-Karaki, M., Mahfouz, Y., Salameh, P., Matta, J., Helou, K., and Narbonne, J. F. (2019). Patterns of PCBs and OCPs exposure in a sample of Lebanese adults: The role of diet and physical activity. *Environ. Res.* **179**, 108789.

Inbal, B., Bialik, S., Sabanay, I., Shani, G., and Kimchi, A. (2002). Dap kinase and drp-1 mediate membrane blebbing and the formation of autophagic vesicles during programmed cell death. *J. Cell Biol.* **157**, 455–468.

Isshiki, K., Hirase, T., Matsuda, S., Miyamoto, K., Tsuji, A., and Yuasa, K. (2015). Death-associated protein kinase 2 mediates nocodazole-induced apoptosis through interaction with tubulin. *Biochem. Biophys. Res. Commun.* **468**, 113–118.

Kang, J. H., Park, H., Chang, Y. S., and Choi, J. W. (2008). Distribution of organochlorine pesticides (OCPs) and polychlorinated biphenyls (PCBs) in human serum from urban areas in Korea. *Chemosphere* **73**, 1625–1631.

Katarzyńska, D., Hrabia, A., Kowalik, K., and Sechman, A. (2015). Comparison of the in vitro effects of TCDD, PCB 126 and PCB 153 on thyroid-restricted gene expression and thyroid hormone secretion by the chicken thyroid gland. *Environ. Toxicol. Pharmacol.* **39**, 496–503.

Klionsky, D. J. (2007). Autophagy: From phenomenology to molecular understanding in less than a decade. *Nat. Rev. Mol. Cell Biol.* **8**, 931–937.

Lee, K., Kim, Y.-J., Cho, Y. Y., Chung, S., Jo, S.-H., and Choi, S.-Y. (2017). Polychlorinated biphenyl 19 blocks the most common form of store-operated Ca(2+) entry through ORAI. *Naunyn-Schmiedeberg's Arch. Pharmacol.* **390**, 1221–1228.

Levin-Salomon, V., Bialik, S., and Kimchi, A. (2014). Dap-kinase and autophagy. *Apoptosis* **19**, 346–356.

Maejima, Y., Isobe, M., and Sadoshima, J. (2016). Regulation of autophagy by beclin 1 in the heart. *J. Mol. Cell. Cardiol.* **95**, 19–25.

Maqbool, F., Mostafalou, S., Bahadar, H., and Abdollahi, M. (2016). Review of endocrine disorders associated with environmental toxicants and possible involved mechanisms. *Life Sci.* **145**, 265–273.

Medina, D. L., and Santisteban, P. (2000). Thyrotropin-dependent proliferation of in vitro rat thyroid cell systems. *Eur. J. Endocrinol.* **143**, 161–178.

Merritt, R. L., and Foran, C. M. (2007). Influence of persistent contaminants and steroid hormones on glioblastoma cell growth. *J. Toxicol. Environ. Health Part A* **70**, 19–27.

Mizushima, N., and Yoshimori, T. (2007). How to interpret lc3 immunoblotting. *Autophagy* **3**, 542–545.

Orrenius, S., Zhivotovsky, B., and Nicotera, P. (2003). Regulation of cell death: The calcium-apoptosis link. *Nat. Rev. Mol. Cell Biol.* **4**, 552–565.

Pessah, I. N., Cherednichenko, G., and Lein, P. J. (2010). Minding the calcium store: Ryanodine receptor activation as a convergent mechanism of PCB toxicity. *Pharmacol. Ther.* **125**, 260–285.

Rudge, C. V. C., Sandanger, T., Röllin, H. B., Calderon, I. M. P., Volpato, G., Silva, J. L. P., Duarte, G., Neto, C. M., Sass, N., Nakamura, M. U., *et al*. (2012). Levels of selected persistent organic pollutants in blood from delivering women in seven selected areas of São Paulo state, Brazil. *Environ. Int.* **40**, 162–169.

Sánchez-Alonso, J. A., López-Aparicio, P., Recio, M. N., and Pérez-Albarsanz, M. A. (2003). Apoptosis-mediated neurotoxic potential of a planar (PCB 77) and a nonplanar (PCB 153) polychlorinated biphenyl congeners in neuronal cell cultures. *Toxicol. Lett.* **144**, 337–349.

Spector, J. T., De Roos, A. J., Ulrich, C. M., Sheppard, L., Sjödin, A., Wener, M. H., Wood, B., and McTiernan, A. (2014). Plasma polychlorinated biphenyl concentrations and immune function in postmenopausal women. *Environ. Res.* **131**, 174–180.

Takaguchi, K., Nishikawa, H., Mizukawa, H., Tanoue, R., Yokoyama, N., Ichii, O., Takiguchi, M., Nakayama, S. M. M., Ikenaka, Y., Kunisue, T., *et al.* (2019). Effects of PCB exposure on serum thyroid hormone levels in dogs and cats. *Sci. Total Environ.* **688**, 1172–1183.

Tang, H. W., and Chen, G. C. (2011). Unraveling the role of myosin in forming autophagosomes. *Autophagy* **7**, 778–779.

Tang, J. M., Li, W., Xie, Y. C., Guo, H. W., Cheng, P., Chen, H. H., Zheng, X. Q., Jiang, L., Cui, D., Liu, Y., *et al.* (2013). Morphological and functional deterioration of the rat thyroid following chronic exposure to low-dose PCB118. *Exp. Toxicol. Pathol.* **65**, 989–994.

Tarkowski, S. (1996). Environmental health in Europe. A who perspective. *Int. J. Occup. Med. Environ. Health* **9**, 1–6.

Tischfield, M. A., and Engle, E. C. (2010). Distinct alpha- and beta-tubulin isotypes are required for the positioning, differentiation and survival of neurons: New support for the 'multi-tubulin' hypothesis. *Biosci. Rep.* **30**, 319–330.

Tornquist, K., Ramstrom, C., Rudnas, B., Klika, K. D., Dugue, B., Adams, J., Zipkin, R., Pihlaja, K., and Pasternack, M. (2002). Ceramide 1-(2-cyanoethyl) phosphate enhances store-operated Ca2+ entry in thyroid frtl-5 cells. *Eur. J. Pharmacol.* **453**, 1–11.

Wassermann, M., Wassermann, D., Cucos, S., and Miller, H. J. (1979). World PCBs map: Storage and effects in man and his biologic environment in the 1970s. *Ann NY Acad. Sci.* **320**, 69–124.

Wen, G., Ringseis, R., and Eder, K. (2017). Endoplasmic reticulum stress inhibits expression of genes involved in thyroid hormone synthesis and their key transcriptional regulators in frtl-5 thyrocytes. *PLoS One* **12**, e0187561.

Xu, B., Yang, H., Sun, M., Chen, H., Jiang, L., Zheng, X., Ding, G., Liu, Y., Sheng, Y., Cui, D., *et al.* (2016). 2,3′,4,4′,5-pentachlorobiphenyl induces inflammatory responses in the thyroid through jnk and aryl hydrocarbon receptor-mediated pathway. *Toxicol. Sci.***149**, 300–311.

Yang, H., Chen, H., Guo, H., Li, W., Tang, J., Xu, B., Sun, M., Ding, G., Jiang, L., Cui, D., *et al.* (2015). Molecular mechanisms of 2,3′,4,4′,5-pentachlorobiphenyl-induced thyroid dysfunction in frtl-5 cells. *PLoS One* **10**, e0120133.

Yang, J., Yu, J., Li, D., Yu, S., Ke, J., Wang, L., Wang, Y., Qiu, Y., Gao, X., Zhang, J., *et al.* (2017). Store-operated calcium entry-activated autophagy protects EPC proliferation via the CAMKK2-MTOR pathway in ox-LDL exposure. *Autophagy* **13**, 82–98.

Zhao, G., Wang, Z., Zhou, H., and Zhao, Q. (2009). Burdens of PBBs, PBDEs, and PCBs in tissues of the cancer patients in the e-waste disassembly sites in Zhejiang, China. *Sci. Total Environ.* **407**, 4831–4837.

Zhou, Q., Wang, L., Chen, H., Xu, B., Xu, W., Sheng, Y., and Duan, Y. (2019). 2,3′,4,4′,5-pentachlorobiphenyl induced autophagy of the thyrocytes via DAPK2/PKD/VPS34 pathway. *Arch. Toxicol.* **93**, 1639–1648.

Zhu, Z. D., Yu, T., Liu, H. J., Jin, J., and He, J. (2018). SOCE induced calcium overload regulates autophagy in acute pancreatitis via calcineurin activation. *Cell Death Dis.* **9**, 50.